© 2022 IEEE. Personal use of this material is permitted. Permission from IEEE must be obtained for all other uses, in any current or future media, including reprinting/republishing this material for advertising or promotional purposes,creating new collective works, for resale or redistribution to servers or lists, or reuse of any copyrighted component of this work in other works. DOI 10.1109/IGARSS46834.2022.9884115

ON ADAPTIVE UNSCENTED KALMAN FILTERING FOR FLOATING DOPPLER WIND-LIDAR MOTION CORRECTION: EFFECT OF THE NUMBER OF LIDAR MEASUREMENT HEIGHTS

A. Salcedo-Bosch[1], *F. Rocadenbosch*[1,2] *Senior member, IEEE, J. Sospedra*[3]

[1]CommSensLab-UPC, Department of Signal Theory and Communications (TSC), Universitat Politècnica de Catalunya (UPC)

[2]Institut d'Estudis Espacials de Catalunya (Institute of Space Studies of Catalonia, IEEC), Barcelona, Spain, E-08034 Barcelona, Spain

[3]Laboratori d'Enginyeria Maritima, Universitat Politècnica de Catalunya, E-08034 Barcelona, Spain

Correspondence: andreu.salcedo@upc.edu (A. S.-B.); francesc.rocadenbosch@upc.edu (F.R.)

ABSTRACT

This work studies the influence of the number of lidar measurement heights on the performance of the floating Doppler wind lidar motion-correction algorithm, recently published by the authors. The work is in the context of offshore wind energy and continuous-wave focusable Zephir^{TM}300 lidar. A down-sampling technique applied over the lidar-measured wind speed time-series is used to simulate different height-sounding configurations. The operation of the filter under one, three, and five measurement heights of the lidar is studied by using data from El Pont del Petroli measurement campaign. The filter is proved to remove apparent turbulence addition in all three cases, showing a deterioration of statistical indicators as the number of sounding heights increase.

Index Terms— DWL, floating, wind profile, Kalman filter, motion correction

1. INTRODUCTION

Doppler Wind Lidars (DWLs) sited on offshore floating platforms or buoys are being accepted in the wind energy (WE) industry as an alternative to costlier meteorological masts (metmasts) [1]. As offshore wind farms are deployed further off-coast and to higher depths, metmasts are not a feasible solution for wind resource assessment [2]. Floating Doppler Wind lidars

This research was funded by the Spanish Government and EU Regional Development Funds, ARS project PGC2018-094132-B-I00, H2020 ACTRIS-IMP project GA-871115 and H2020 ATMO-ACCESS project GA-101008004. The European Institute of Innovation and Technology (EIT), KIC InnoEnergy project NEPTUNE (call FP7) supported the measurement campaigns. The Generalitat de Catalunya—AGAUR funded doctoral grant 2020 FISDU 00455 by A. Salcedo-Bosch. CommSensLab-UPC is an Excellence Unit (MDM-2016-0600) funded by the Agencia Estatal de Investigación, Spain.

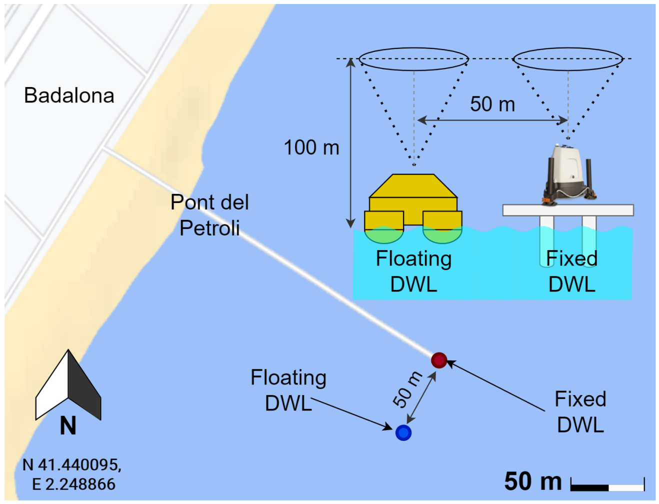

Fig. 1. El Pont del Petroli campaign location and scheme of the instrumental set-up. Adapted from [5].

(FDWLs) are able to reliably measure the mean horizontal wind speed (HWS) and wind direction (WD) at a ten-minute level in a more flexible and cost-effective manner [3]. However, the wave-motion effect over the FDWL buoy induces an error on the lidar-measured wind vector and turbulence intensity (TI). TI is defined as the ratio between the standard deviation of the HWS (σ_{HWS}) to the mean HWS. In comparison to the anemometers sited on metmasts, which measure "true" point-wise TI, DWLs measure an apparent TI as a consequence of the lidar probe length (spatial average) and temporal average inherent to the DWL measurement algorithm. Moreover, the wave-induced buoy motion causes an apparent turbulence addition to the TI measurements by FDWLs in comparison to fixed DWLs. [4].

Correct assessment of the TI is of main importance for the industry because overestimation of the TI may lead to wind turbine over-design and extra costs. Therefore, compensation of the FDWL motion-induced error in wind-vector measurements is an active topic of research in the state of the art. So far, different methodologies have been presented towards this purpose, which either require access to the lidar internal line-of-sight (LoS) measurements [2] or to carry out the compensation statistically at a post-processing level [6]. Recently, an on-the-run FDWL motion-correction method which does not require accessing the lidar internal LoS measurements has been presented by the authors [5]. The method is based on an adaptive Unscented Kalman Filter (UKF) that takes into account the FDWL dynamics as well as the lidar wind-retrieval algorithm to estimate the motion-corrected wind vector. The filter was validated using experimental data from El Pont del Petroli (PdP) campaign, in which two identical lidars, one floating and one fixed, the latter used as reference, were configured to measure the wind at a single height of 100 m above sea level. However, in practice, continuous-wave, focusing DWLs are usually set up to measure the wind profile by sequentially sounding the wind at multiple heights. In this paper we present a methodology to simulate the measurement height configuration by down-sampling the lidar-measured wind-vector time-series and we assess the performance of the FDWL motion-correction UKF in relation to the number of measurement heights chosen.

2. MATERIALS AND METHODS

2.1. Materials

The PdP experimental campaign took place in June 2013. In the campaign, the NEPTUNE proof-of-concept FDWL buoy was tested against a reference fixed lidar sited 50 m away at El Pont del Petroli pier (Badalona, Spain, see Figure 1). Both the fixed DWL and the FDWL were identical Zephir^{TM}300 models, calibrated on-shore and user-configured to measure the wind vector at 100 m. The Zephir^{TM}300 is a continuous-wave focusable DWL measuring at a rate of 1 scan/s (50 LoS/scan) at any given height and with 10 user-configurable measurement heights. The FDWL buoy hosted two inertial measurement units (IMUs) to measure the buoy and lidar attitudes, i.e., 6-Degrees of Freedom (DoF) motion.

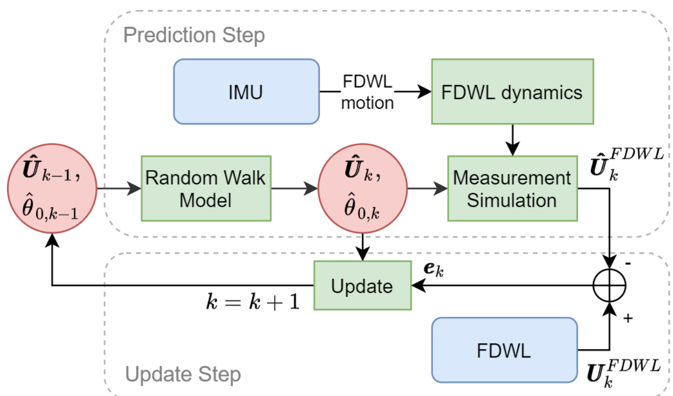

Fig. 2. Block diagram depicting the motion-correction UKF recursive algorithm.

2.2. Methods

2.2.1. Review of the FDWL motion-correction filter

The UKF takes advantage of the knowledge of FDWL dynamics as formulated by Kelberlau et al. [2] as well as the lidar internal wind-retrieval algorithm to recursively estimate the "clean" (i.e., motion-free) wind vector $\hat{\boldsymbol{U}}_k$ and lidar initial scan phase $\hat{\theta}_{0,k}$ at each discrete time k. The filter uses the FDWL-measured wind vector $\boldsymbol{U}_k^{FDWL}$ and the FDWL 6-DoF motion measurements by the IMUs on the buoy to carry out the estimation. Figure 2 depicts the FDWL motion-correction UKF block diagram. Each recursive loop of the filter consists of the following prediction and update steps (refer to [5] for further insight in the filter):

Prediction step:

1. "A priori" predict present-time $\hat{\boldsymbol{U}}_k$ and $\hat{\theta}_{0,k}$ from previous $\hat{\boldsymbol{U}}_{k-1}$ and $\theta_{0,k-1}$ by assuming a random-walk model.
2. Predict present-time FDWL-measured wind vector $\hat{\boldsymbol{U}}_k^{FDWL}$ given $\hat{\boldsymbol{U}}_{k-1}$ and $\hat{\theta}_{0,k-1}$ by considering the lidar wind-retrieval algorithm and buoy-motion attitude (IMU measured).

Update step:

1. Compute the measurement estimation error $\boldsymbol{e}_k$ as the difference between the estimated $\hat{\boldsymbol{U}}_k^{FDWL}$ and actual FDWL measurement $\boldsymbol{U}_k^{FDWL}$.

2. "A posteriori" update the predicted $\hat{\boldsymbol{U}}_k$ and $\hat{\theta}_{0,k}$ as a function of $\boldsymbol{e}_k$.

2.2.2. *Emulation of the DWL height-measuring configuration*

Continuous-wave focusing DWLs measure the wind at multiple heights sequentially and, therefore, this means that *they sound a particular height every n scans* ($\simeq$1 scan/s), with n the number of measurement heights. When a lidar is configured to measure at multiple heights, this is equivalent to down-sampling (DS) the wind-vector time-series by a factor n,

$$\boldsymbol{U}^{DS:n}[k] = \boldsymbol{U}[n \cdot k], \tag{1}$$

where $\boldsymbol{U}[k]$ is the wind-vector time-series and $\boldsymbol{U}^{DS:n}[k]$ is the down-sampled version by a factor n. Figure 3a shows an example of the HWS time-series measured by the FDWL and the fixed DWL. The fixed-DWL time-series is shown along with its factor-3 and factor-5 down-sampled versions, which emulates 3- and 5-height sounding configurations, respectively.

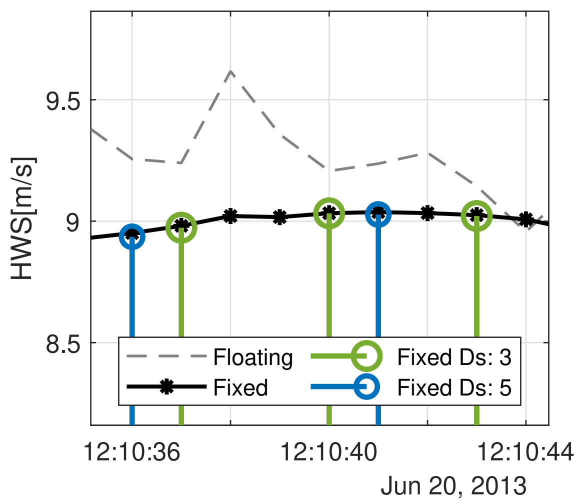

Fig. 3. Example of the HWS time-series measured by the FDWL (dashed gray trace) and the fixed DWL (black trace) at the 100 m in height (single measuring height). The fixed-DWL time-series is shown along with its down-sampled versions by a factor of 3 (green samples) and 5 (blue samples).

3. RESULTS AND DISCUSSION

As it can be observed in Figure 3, the instantaneous HWS measurements by the fixed DWL and FDWL are not identical since the instruments were 50 m apart. In order to study the UKF motion-correction performance, the TIs measured by the FDWL ($TI_{Float.}$) at the *single measuring height* of 100 m, with and without correction, were compared (at 10-minute resolution) against the TIs measured by the reference fixed DWL (TI_{Fixed}) considering three measurement-height configurations: (i) single-height sounding, and (ii) 3, and (iii) 5 sounding heights. Cases (ii) and (iii) were emulated by inputting to the filter factor-3 and -5 downsampled time-series, respectively).

Figure 4 shows three scatter plots comparing the TI measured by the FDWL (with and without motion correction) and the fixed DWL as a function of the number of lidar measurement heights (panels a-c). Numerical analysis yielded three statistical indicators for each measurement height: coefficient of determination (R^2), Root-Mean-Squared Error (RMSE) and Linear Regression line (LR).

The RMSE is defined as

$$RMSE = \sqrt{\frac{\sum_{i=1}^{N}(TI_{Float.,i} - TI_{Fixed,i})^2}{N}}, \tag{2}$$

where N is the number of 10-min samples of the 24 hour period under study.

On one hand, Figure 4 shows at a glance that without motion correction and irrespective of the number of measurement heights chosen, the huge majority of TI measurements by the FDWL, $TI_{Float.}$, fall above the ideal 1:1 line. This bias evidences the additive TI due to buoy motion. After correction, the scatter points shifted down to virtually lay along the ideal 1:1 line, showing noticeable bias reduction between the TI measured by the fixed and the FDWL. This is evidenced by red LR lines, virtually overlapping the ideal 1:1 line in all three panels, which demonstrates effective motion correction by the UKF. Quantitatively, LR offset values, which are indicative of the average additive turbulence caused by wave motion, greatly reduced from $\simeq$2% (uncorrected) to -0.14% (corrected) when measuring at 1 height (panel a)), and to -0.4% when measuring at 3 and 5 heights (panels b), and c), respectively).

On the other hand, increasing the number of sounding heights caused the TI points to scatter more widely. Specifically, when measuring at a single height (Figure 4 a)), a one-to-one point correspondence was found for most of the points lying not further than 1% bias from the 1:1 line whereas when measuring at 5 heights (Figure 4 c)), many points lay further than 2% bias from the 1:1 line. Consequently, the determination coefficient, R^2, reduced from an almost ideal value, $R^2 = 0.94$, when measuring at a single height, to $R^2 = 0.88$ and $R^2 = 0.81$ when measuring at 3 and 5 heights, respectively. Regarding the RMSE, it increased from 0.74%, when the lidar measured at a single height, to 1.03% and 1.34% when the lidar measured at 3 and 5 heights, respectively. The poorer one-to-one-point correspondence attained for increasing measurement height numbers (equivalently, lower sampling rates in the simulation) stated that less wind information was retained in the 10-min time-series. This is to say that the number of samples in a 10-min segment reduces by a factor equal to the number of measurement heights. Under these circumstances, the filter may face an observability problem in which the measurements no longer provide enough information for the filter to properly estimate the state variables [7]. Besides, as fewer and fewer samples become available in the 10-min time-series, the filter convergence time increases.

In turn, when comparing DWL measuring at a single height to point-like measurements such as those coming up from anemometers, DWLs inherently smooth out small turbulence scales (i.e., high-frequency time-series variations) on account of

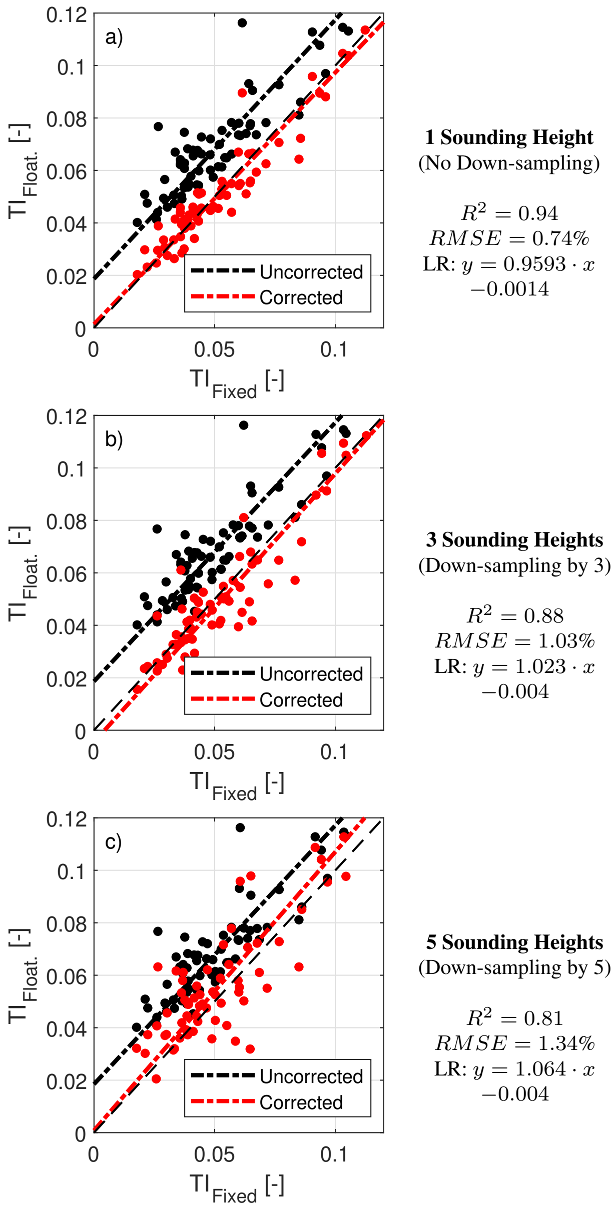

Fig. 4. Scatter plots comparing the TI measured by the FDWL with/without motion correction (red/black dots) and the reference fixed lidar as a function of sounding heights number (panels a-c), 20 June 2013. Color-coded dot-dashed lines represent the linear regressions (LR) of the measurement sample. (Dashed black lines) Ideal 1:1 line. TI_{Fixed} and $TI_{Float.}$ denote the fixed-DWL- and FDWL-measured turbulence intensity.

the spatial and temporal average imposed by the conical scanning pattern at a given height and focusing length [8].

4. CONCLUSIONS

A study on the FDWL motion-correction performance when using the UKF method [5] and in relation to the number of lidar measurement heights (Zephir^{TM}300) was presented. It was shown that, at a given height, the effect of sequentially measuring at N different heights is equivalent to down-sampling the wind vector at that height by the same factor. The TI measured by the

FDWL, with and without motion-correction, was compared against the TI measured by the fixed DWL for three configurations (1, 3, and 5 measurement heights).

The experimental results successfully showed that the filter was able to take the sea motion out of the wind speed measurements, hence to virtually remove the apparent turbulence induced by wave motion for all three height measurement configurations. Numerical analysis also showed that statistical indicators deteriorated as the number of sounding heights increased. Thus, the coefficient of determination reduced from $R^2 = 0.94$ (1 height) to 0.81 (5 heights), and the RMSE increased from 0.74% (1 height) to 1.34% (5 heights).

Future work plans to validate the quantitative statistical indicators retrieved by the UKF simulator with reference to experimental wind-speed data measured under real conditions.

5. REFERENCES

[1] Carbon Trust, "Carbon Trust Offshore Wind Accelerator Roadmap for the commercial acceptance of floating LiDAR technology," Tech. Rep., Carbon Trust, Oct. 2018.

[2] Felix Kelberlau, Vegar Neshaug, Lasse Lønseth, Tania Bracchi, and Jakob Mann, "Taking the motion out of floating lidar: Turbulence intensity estimates with a continuous-wave wind lidar," *Remote Sens.*, vol. 12, no. 5, 2020.

[3] Y. L. Pichugina, R. M. Banta, W. A. Brewer, S. P. Sandberg, and R. M. Hardesty, "Doppler lidar–based wind-profile measurement system for offshore wind-energy and other marine boundary layer applications," *J. Appl. Meteorol. Climatol*, vol. 51, pp. 327–349, Feb. 2011.

[4] A. Salcedo-Bosch, M. A. Gutierrez-Antunano, J. Tiana-Alsina, and F. Rocadenbosch, "Floating Doppler wind lidar measurement of wind turbulence: a cluster analysis.," in *2020 IEEE Int. Geosci. Remote Se. (IGARSS-2020)*, Virtual Event, 2020, IEEE.

[5] Andreu Salcedo-Bosch, Francesc Rocadenbosch, and Joaquim Sospedra, "A robust adaptive unscented kalman filter for floating doppler wind-lidar motion correction," *Remote Sens.*, vol. 13, no. 20, 2021.

[6] Miguel Gutiérrez-Antuñano, Jordi Tiana-Alsina, Andreu Salcedo, and Francesc Rocadenbosch, "Estimation of the Motion-Induced Horizontal-Wind-Speed Standard Deviation in an Offshore Doppler Lidar," *Remote Sens.*, vol. 10, no. 12, pp. 2037, dec 2018.

[7] Robert Robert Grover and Patrick Y.C. Hwang, *Introduction to Random Signals and Kalman Filtering: with MATLAB exercises*, Wiley, 4 edition, 2012.

[8] Ameya Sathe, *Estimating Turbulence Statistics and Parameters from Lidar Measurements. Remote Sensing Summer School*, Number 0085 in DTU Wind Energy E. DTU Wind Energy, Denmark, 2015.